Characterisation of Air-in-water Upward Flows with Electrical Impedance Tomography and Wire Mesh Sensor

J. Jia[a], M. Wang[a], Y. Faraj[a], J. Zhang [b] and X. Yu[c]

[a]*Univ. Leeds, Institute of Particle Science and Engineering, Clarendon Rd, LS2 9JT, Leeds, UK*
[b]*Institute Institute of Mechanics, Chinese Academy of Sciences, Beijing, 100190, China*
[c]*State Key Lab. of Oil and Gas Reservoir Geology and Exploitation, Southwest Petroleum University, Chengdu, 610500, China*

Abstract

Both Electrical Impedance Tomography (EIT) and Wire-Mesh Sensor (WMS) can present the characterisation of air-in-water upward flows, for instance *in-situ* volumetric fraction and velocity of air phase. The performance of EIT with linear back projection (LBP) algorithm and WMS was compared in the previous research. In this study, the same EIT measurement data were off-line processed with the sensitivity theorem based inverse solution using conjugate gradients method (SCG), which is an iterative algorithm. In two flow regimes, air void fraction and air velocity produced by LBP and SCG method in EIT are investigated against WMS.

Keywords: image processing; β grain boundary; X-ray microtomography; lamellar microstructure

1. Introduction

To develop an advanced measurement and visualisation metering technique for two or three phase flows, the characteristics of the flows have to be known due to the great impact of the complexity and discontinuity of disperse phase flow regime on measurement linear range. Electrical Impedance Tomography (EIT) is a non-intrusive tool to disclose the characterisation of two or three phase flow. It has very good temporal resolution but low spatial resolution. Linear Back Projection algorithm (LBP) is a common method to reconstruct the cross-sectional images of the sensing plane for on-line measurement, because of the simply mathematical computation. The iterative methods can optimise the image quality but their computation takes much longer time than LBP. Wire-Mesh Sensor (WMS) [1] is an intrusive tomographic modality and it is an excellent tool to calibrate other tomographic modalities [2]. Like EIT, WMS also can provide the local air void fraction on each crossing points of two groups of perpendicular wires. Integrating all the local air void fraction results in the mean air volumetric void fraction. WMS is able to provide air velocity distribution and mean air velocity using cross-correlation algorithm too. The sensitivity theorem based inverse solution using conjugate gradients methods (SCG) was developed [3]. This is an iterative algorithm and can significantly improve the quality of the individual reconstructed image. It is interesting to investigate whether SCG can further improve the accuracy of EIT's flow measurement against WMS.

1.1 LBP

Linear Back Projection algorithm (LBP) [4] builds the approximate relationship between the relative conductivity change and the relative voltage change in Equ. (1).

$$\frac{\sigma-\sigma_o}{\sigma_o} \approx -\frac{V-V_o}{V_o} \times S \qquad (1)$$

Where S is the normalised sensitivity matrix. When the pipeline is full of single phase, water in this case, σ_0 is the conductivity array of all the pixels cross the cross-sectional sensing area. V_o is the voltage array taken by

EIT system. σ is the conductivity of mixture and *V* is the voltage array when air-in-water mixture is flowing along the pipeline. Equ. (1) is further simplified as Equ. (2) to obtain the mixture conductivity array σ, which then is mapped to the different colour to image the distribution of air and water. Based on Equ. (2), the air void fraction on each pixel of the reconstructed image and air velocity are derived by Maxwell equation [5] and cross-correlation algorithm respectively.

$$\sigma \approx \sigma_o \cdot (1 - \frac{V - V_o}{V_o} \times S) \tag{2}$$

1.2. SCG

The sensitivity theorem based inverse solution using conjugate gradients method (SCG) is an iterative algorithm. The computing procedure of SCG algorithm is illustrated in Fig. 1. The initial measured voltages of EIT system is fed into the Pro-process section. In the inverse solution section, the conjugate gradients (CG) method [3] searches for a minimised residual between the measured and simulated voltages by applying a number of iterations. The use of CG with controlled iterations in each linear inverse step can produce an optimised approximation for solving the non-linear problem with multi-steps. The forward solution produces an error vector for the inverse solution in each step. The sensitivity matrix is also updates in this section for the inverse solution in the next step. Either the number of iteration or the level of error can be set to stop iteration process. Finally, the optimised mixture conductivity array is delivered from Post-assembly for the later computation of air void fraction and air velocity.

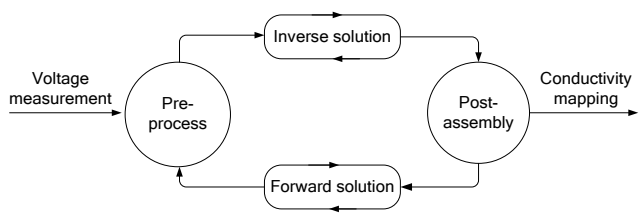

Fig. 1. Computing procedure of SCG algorithm.

2. Methodology

2.1. Experiment setup

A group of experiments were carried out on an air-in-water two-phase flow loop in the University of Leeds. The sketch of the flow loop is shown in Fig. 2. To ensure the flow condition consistent, EIT and WMS were positioned only 22.5 cm apart from a point midway between the centre of the EIT's two planes and the centre of the WMS's two planes. The EIT system worked in the block acquisition mode without on-line displaying the reconstructed images. The maximum frame number acquired at one block was 8000 frames. In this study, 8000 frames per one block acquisition were set up for EIT and speed was 896 dual frames per second, which took approximately 9 seconds. In order to set two modalities run simultaneously, the measurement frequency of the WMS was set as 1024 dual frames per second, which was close to the speed of EIT. More detailed experimental setups were described in the literature [6].

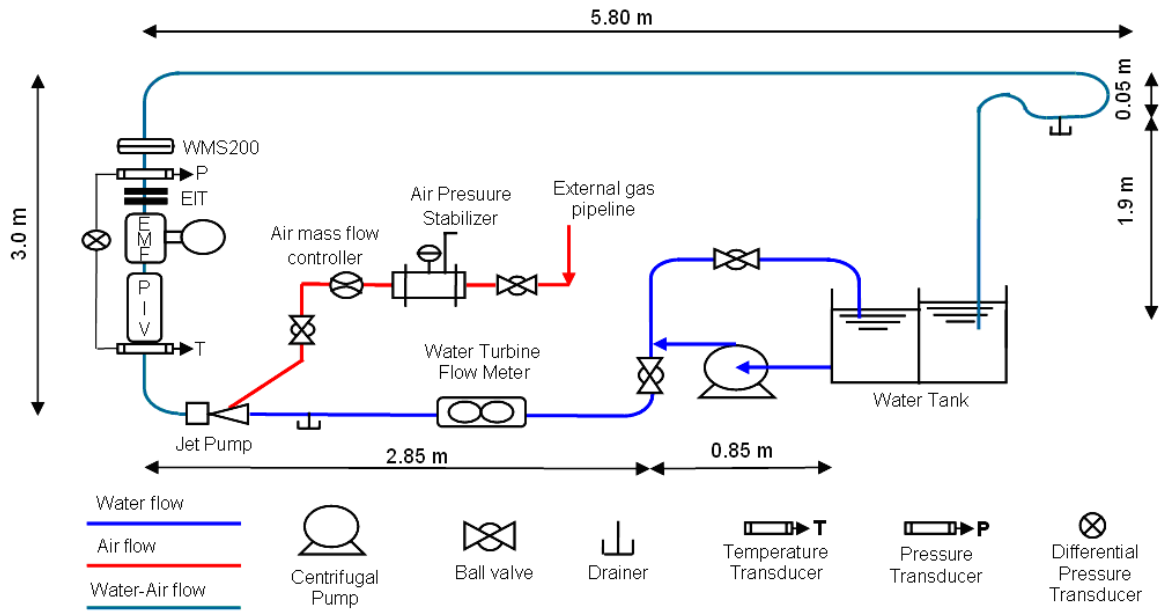

Fig. 2. Sketch of the experimental flow loop.

2.2. Air void fraction

Following Equ. (2), the local void fraction of each image pixel α is derived from Maxwell equation below [5] with measured σ and σ_o by EIT.

$$\alpha = \frac{2\sigma_o - 2\sigma}{\sigma + 2\sigma_o} \tag{3}$$

The local void fraction on each crossing point of WMS is deduced from the relative difference between the measured voltages of pure water flow and the voltages of two phase flow. In Fig. 3, the mean air void fractions from EIT and WMS are plotted. As shown on the blue triangle points, in the bubble flow regimes, a good agreement between the EIT and the WMS is displayed. However, a gradual discrepancy under slug flow regime is revealed on the red square points. Compared with WMS, EIT tends to underestimate the overall air void fraction, particularly when the mean air void fraction is over 25%. The deviation between two systems has a linear relation, which facilitates the calibration for EIT.

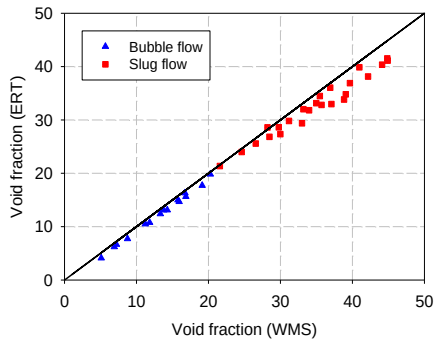

Fig. 3. Comparison of overall air void fraction between EIT and WMS.

2.3. Air velocity

In EIT, the local air velocity is resulted from the two corresponding local conductivity values on the two electrode sensing planes. AMIFlow cross-correlation software was used to process the conductivity distribution and generate the information of air velocity. In WMS, the signals from both measurement planes of WMS are cross-correlated separately for each pair of mesh points, which are located above each other. WMS uses the Fast Fourier Transformation to make a fast cross-correlation between the data of two sensors in flow direction. The technique of averaging the cross-correlation functions before searching for the maximum has proven to supply more stable velocity values than if the velocities were directly deduced from the result of a point-to-point cross-correlation [7].

3. Results

Two sets of EIT and WMS data representing two typical flow regimes are selected and reprocessed using SCG method. When the water flow rate before mixing is 2.04×10^{-3} m^3/s and air flow rate is 2.50×10^{-4} m^3/s and the superficial velocity of water and air are 1.039 m/s and 0.127 m/s respectively, which determined that the flow belongs to the bubble flow regime. When the water flow rate before mixing is 4.11×10^{-4} m^3/s and air flow rate is 9.17×10^{-4} m^3/s and the superficial velocity of water and air are 0.209 m/s and 0.465 m/s respectively, which determined that the flow belongs to the slug flow regime.

3.1. Bubble flow regime

3.1.1. Air void fraction profile

The local air void fractions around the concentric circle from the image boundary to the center are averaged. All averaged values representing each concentric circle form a symmetrical radial air void fraction profile. Three local air void fraction profiles are shown in Fig. 4. The blue profile of LBP has large difference with that of WMS. In contrast, the wall peak pattern [8] is clearly displayed on the black WMS's profile but not on the LBP's profile. The same EIT raw data are reprocessed using SCG algorithm. Its red profile slightly rises up around the pipe wall, but the whole profile is more similar with that of LBP rather than WMS.

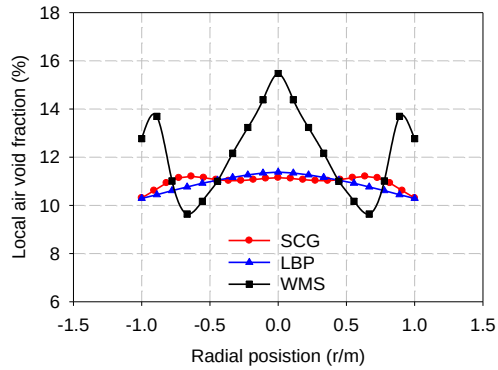

Fig. 4. Local air void fraction profiles, V_{sw}=1.039 m/s, V_{sa} = 0.127 m/s.

3.1.2. Air velocity profile

The air velocity profile is created in the same way like air void fraction profile. As shown in Fig. 5, all three velocity profiles have smooth shape. The air velocity on the center of the pipe is larger than that on the boundary on the pipe. The velocity profile given by WMS has a relative flat crest curve. WMS is an intrusive sensor to flow especially for the velocity calculation. It could have resistance effect to the air bubbles. The shape of the air velocity profiles from LBP and SCG are similar, but the larger air velocity on the center of the pipe is presented on the profile produced by SCG.

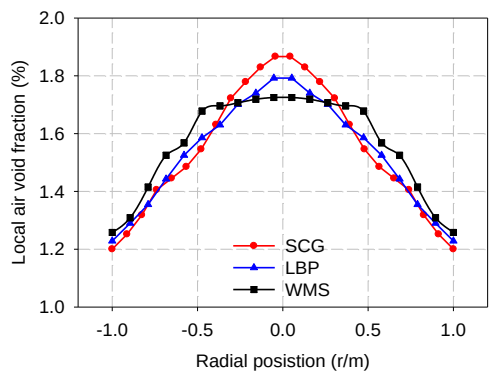

Fig. 5. Local air velocity profiles, V_{sw}=1.039 m/s, V_{sa} = 0.127 m/s.

3.1.3. Mean air void fraction and mean velocity

When the flow regime is bubble flow and the air void fraction is relatively low. The mean air void fraction and mean air velocity shown in Table 1 indicate that SCG does not significantly improve the results based on LBP.

Table 1. Mean air void fraction and velocity in bubble flow regime

	Mean air void fraction (%)	Mean air velocity (m/s)
WMS	11.836	1.446
EIT-LBP	10.719	1.426
EIT-SCG	10.890	1.415

3.2. Slug flow regime

3.2.1. Air void fraction profile

The local air void fraction profiles are shown in Fig. 6. The core peak pattern [7] is both displayed on the WMS's and LBP's profile. But the local air void fraction of WMS is flatter than that of LBP. Moreover, the profile of LBP is drifted down. The same raw data are reprocessed using SCG algorithm. The new profile is more similar with that of WMS rather than LBP.

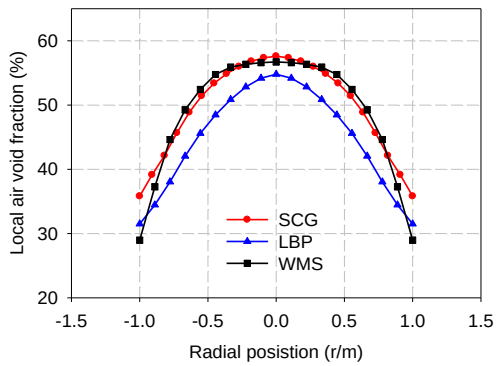

Fig. 6. Local air void fraction profiles, V_{sw}=0.209 m/s, V_{sa} = 0.465 m/s.

3.2.2. Air velocity profile

When the water flow rate is low and the air flow rate is high, the flow is more turbulent. The velocity measurement from EIT is not very accurate, because the cross-correlation calculation is based on the assumption the air is along the upwards axial direction. But in fact, the air bubbles could travel different directions.

In Fig. 7, the black velocity profile from WMS has flat distribution. However, the blue velocity profile of LBP shows the air around the pipe wall has a dramatically velocity increase, which is believed due to the systemic error. The SCG can correct this error, but compared with the air velocity of WMS, the red velocity profile of SCG still have a positive offset.

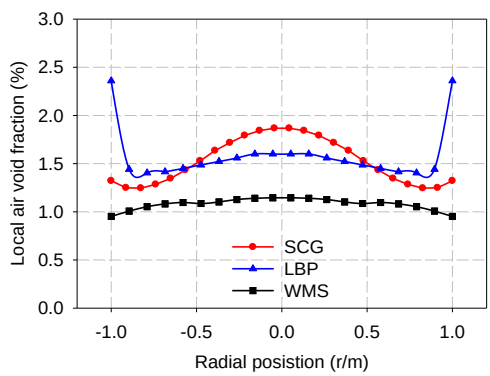

Fig. 7. Local air velocity profiles, V_{sw}=0.209 m/s, V_{sa} = 0.465 m/s.

3.2.3. Mean air void fraction and mean velocity

In Table 2, dislike in the bubble flow regime, SCG is able to deliver mean air void fraction and velocity which has a better agreement with the corresponding results of WMS. Due to two large points on the edge of LBP's velocity profile, mean air velocity is enlarged incorrectly.

Table 2. Mean air void fraction and velocity in slug flow regime

	Mean air void fraction (%)	Mean air velocity (m/s)
WMS	44.127	1.116
EIT-LBP	40.872	1.629
EIT-SCG	45.909	1.395

4. Conclusions

When the flow regime of air-in-water flow is bubble flow, the air void fraction and air velocity were not obviously affected by SCG algorithm. When the flow regime of the flow is slug flow, SCG only can make the air void fraction more close to these of WMS, but not the air velocity. The performance of the SCG relies on the configurations of the parameters. The iterative computation of SCG takes large amount of time to finish. Unless the single-step SCG method can developed to exponential reduce the computational time, it is not feasible to use SCG for on-line EIT measurement. Even LBP underestimates the air void fraction, the rapid calculation speed makes this method the only option for the real-time measurement. The accuracy of the individual frame may not be very good, but after averaging 8000 frames, the random error of the measurement is filtered out. The systematic error caused by the LBP becomes more evident when the air void fraction is increasing, but it can be calibrated. For real-time measurement, LBP still is the best option for image reconstruction method with the respect of calculation speed and accuracy. After all, WMS is an intrusive sensor and could inherently affect its measurement particularly for the velocity calculation.

References

[1] Prasser, H.-M., Böttger, A. and Zschau, J., 1998. A new electrode-mesh tomograph for gas–liquid flows, Flow Measurement and Instrumentation, Vol. 9, Issue 2, pp. 111-119

[2] Prasser, H. -M., Misawa, M. and Tiseanu, I., 2005. Comparison between wire-mesh sensor and ultra-fast X-ray tomography for an air–water flow in a vertical pipe, Flow Measurement and Instrumentation 16, pp. 73–83.

[3] Wang, M., 2001. Inverse solutions for electrical impedance tomography based on conjugate gradients methods, Measurement Science and Technology Vol. 13, Issue 1, pp. 101-117

[4] Kotre, C. J., 1994. EIT image reconstruction using sensitivity weighted filtered back-projection, Physiological Measurement. 15 A, pp.125–136

[5] Maxwell, J. C. A, 1954. Treatise on Electricity and Magnetism, Unabridged Third edition, Vol. 1, Dover Publications Inc. New York.

[6] Olerni, C., Jia, J. and Wang, M., 2013. Measurement of air distribution and void fraction of an upward air-water flow using electrical resistance tomography and wire-mesh sensor, Measurement Science and Technology Vol. 24, No. 3.

[7] Teletronic Rossendorf GMBH 2009 Wire-mesh Sensor System WMS200 Version 1.2 – User's Manual, Radeberg, Germany: Teletronic Rossendorf GmbH.

[8] Seriszawa, A. and Kataoka, I., 1992. Dispersed Flow – Proceeding at the 3rd International Workshop on Two-Phase Flow Fundamentals, June 15–19, London, UK